# Magnetic and magnetothermal tunabilities of subwavelength-hole arrays in a semiconductor sheet

Jiaguang Han,[1] Akhlesh Lakhtakia,[2,*] Zhen Tian,[3,4,5] Xinchao Lu,[3] and Weili Zhang[3]

[1]*Department of Physics, National University of Singapore, 2 Science Drive 3, Singapore 117542, Singapore*
[2]*Department of Engineering Science and Mechanics, Pennsylvania State University, University Park, Pennsylvania 16802, USA*
[3]*School of Electrical and Computer Engineering, Oklahoma State University, Stillwater, Oklahoma 74078, USA*
[4]*Center for Terahertz Waves and College of Precision Instrument and Optoelectronics Engineering, Tianjin University, Tianjin 300072, China*
[5]*Key Laboratory of Opto-electronics Information and Technical Science, Ministry of Education, Tianjin 300072, China*
**Corresponding author: akhlesh@psu.edu*

Received February 9, 2009; revised March 9, 2009; accepted March 12, 2009;
posted April 9, 2009 (Doc. ID 107365); published April 30, 2009

In the low-terahertz regime, the resonance frequency of an array of subwavelength holes in a semiconductor sheet can be doubled or more by isothermally increasing the magnitude of a dc magnetic field, by increasing the temperature in the presence of a constant dc magnetic field, and by increasing both the temperature and the dc magnetic field magnitude. © 2009 Optical Society of America

*OCIS codes:* 050.6624, 160.6000, 260.0260.

Transmission by an electrically small circular hole in a metal plane is very weak [1,2], but transmission by an array of electrically small holes in the same plane can be very strong, as has now been shown experimentally [3] and theoretically [4] in the optical regime. This fascinating phenomenon—sometimes called extraordinary optical transmission—is often explained in terms of the resonant excitation of surface plasmons [5,6]. Arrays of subwavelength holes have shown promising applications in nanofabrication, biochemical sensing, and integrated plasmonic devices [4–8].

The effect of the electromagnetic constitutive properties of the metal can be significant [9]. The choice of the metal and the geometric parameters fixes the resonances of the array. Its usefulness would be considerably enhanced, if the resonances could be tuned after fabrication. The tunability strategies investigated thus far mostly involve either altering the ambient permittivity [10,11] or flooding the holes with electro-optic materials [12]. If the metal is replaced with a doped semiconductor, then a temperature change affects the free-carrier density and thus the resonances [13]; likewise, photoexcitation also leads to tunability [14].

The relative permittivity tensors of certain metals, semiconductors, and liquid crystals can be controlled by the application of a dc magnetic field. Strelniker *et al.* [15,16] adopted quasi-static approaches to homogenize a metal sheet with a subwavelength-hole array into a homogeneous sheet of an equivalent medium. They showed that the equivalent medium's relative permittivity tensor can be controlled by a dc magnetic field.

A semiconductor affords better prospects for tunability in the low-terahertz regime than a metal. We introduce here the magnetothermal modality of tuning the resonance frequency of a subwavelength-hole array in a semiconductor sheet. If a dc magnetic field is applied to alter the relative permittivity tensor of the semiconductor, then, instead of surface plasmons, we have surface magnetoplasmons. In lieu of a dc magnetic field, an appropriate change in temperature will also affect the semiconductor and thus the optical response of the array. Finally, both magnetic and thermal tunabilities can be combined into magnetothermal tunability. To our knowledge, this is the first time that the combination of two modalities for tuning the response of a subwavelength-hole array has been demonstrated.

We chose a 200-nm-thick InSb sheet perforated by a subwavelength-hole array, and the semiconductor sheet is supported by an isotropic Teflon substrate. Undoped InSb is an isotropic $n$-type semiconductor. Its relative permittivity obeys the Drude model [17]. The holes were chosen to be squares of side 24 $\mu$m. The Teflon substrate of relative permittivity $\varepsilon_S = 2.08$ was chosen to be 200 $\mu$m thick. The sides of the holes were oriented parallel to the $y$ and $z$ axes of the Cartesian coordinate system. The lattice was also square, with a period $a_0 = 60$ $\mu$m along both the $y$ and the $z$ axes, as illustrated in the inset of Fig. 1. The lattice period was chosen so that all nonspecular reflection and transmission modes are evanescent in the 1.5–3.5 THz regime, when a plane wave is normally incident on the chosen structure.

We first calculated the reflection coefficient $r$ and the transmission coefficient $t$ of the chosen structure, when a plane wave was normally incident with its electric field parallel to the $z$ axis. We chose a Voigt configuration wherein the dc magnetic field $\mathbf{B_0}$ is aligned perpendicular to the wave vector of the incident plane wave [18]. We also chose $\mathbf{B_0}$ to be aligned perpendicular to electric field of the incident plane wave (i.e., $\mathbf{B_0} \| y$). The computer simulation of the spectral response of the chosen structure was per-

 

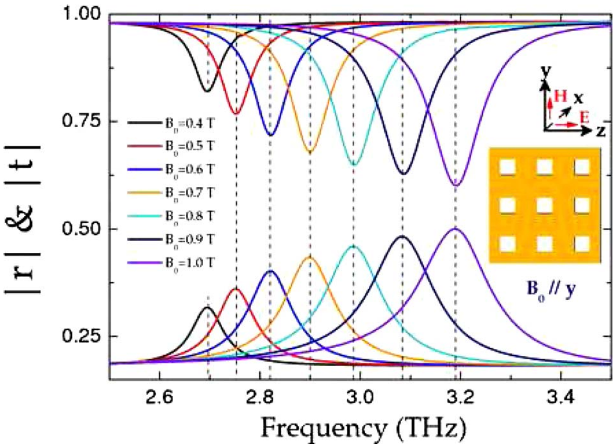


Fig. 1. (Color online) Simulated $B_0$-dependent spectra of $|r|$ (lower) and $|t|$ (upper) of the chosen structure shown in the inset. Because of loss in the semiconductor, $|r|^2+|t|^2 < 1$.

formed using the commercial software CST MICROWAVE STUDIO. Quasi-static approaches were not adopted, because the side of each hole is more than 10% of the free-space wavelength in the 1.5–3.5 THz regime.

For the chosen Voigt configuration, the relative permittivity of InSb is a tensor [19], i.e.,

$$\hat{\varepsilon}(\omega)=\begin{pmatrix}\varepsilon_{xx}(\omega) & 0 & \varepsilon_{xz}(\omega)\\ 0 & \varepsilon_{yy}(\omega) & 0\\ \varepsilon_{zx}(\omega) & 0 & \varepsilon_{zz}(\omega)\end{pmatrix}, \qquad (1)$$

where $\varepsilon_{xx}=\varepsilon_{zz}=\varepsilon_\infty-\omega_p^2(\omega^2+i\gamma\omega)[(\omega^2+i\gamma\omega)^2-\omega^2\omega_c^2]^{-1}$, $\varepsilon_{yy}=\varepsilon_\infty-\omega_p^2(\omega^2+i\gamma\omega)^{-1}$, and $\varepsilon_{zx}=-\varepsilon_{xz}=i\omega\omega_c\omega_p^2[(\omega^2+i\gamma\omega)^2-\omega^2\omega_c^2]^{-1}$. Here, $\varepsilon_\infty$ is the high-frequency value; the plasma frequency $\omega_p=\sqrt{Ne^2/\varepsilon_0 m^*}$ depends on the carrier density $N$, the effective mass $m^*$, the electronic charge $e$, and the free-space permittivity $\varepsilon_0$; $\gamma$ is the damping constant; and $\omega_c=eB_0/m^*$ is the cyclotron frequency. At room temperature (300 K), the following parameters were used in our simulations [20]: $\varepsilon_\infty=15.68$, $N=1.96\times10^{16}\ \mathrm{cm}^{-3}$, $m^*=0.015\ m_e$, and $\gamma/2\pi=0.05$ THz, where $m_e$ is the electron's rest mass.

Figure 1 presents the simulated spectral response of the chosen structure for different values of the magnitudes $B_0$ of $\mathbf{B_0}$. The resonance frequency characterized by the peak in $|r|$ or dip in $|t|$ significantly blueshifts from 2.69 to 3.20 THz as $B_0$ is increased from 0.4 to 1.0 T. The blueshifting with increasing $B_0$ is consistent with quasi-static results [15]. In addition, by increasing $B_0$, the resonance itself is enhanced, as can be gathered from the higher peaks and the deeper dips. As shown in the inset of Fig. 2, the $|r|$ peak increases from 0.32 to 0.50 as $B_0$ varies from 0.4 to 1.0 T, and simultaneously the $|t|$ dip deepens from 0.83 to 0.60.

In a semiconductor hole array under an external dc magnetic field, surface magnetoplasmons are resonantly excited at the semiconductor–dielectric interface (i.e., the InSb–Teflon interface) to conserve mo-

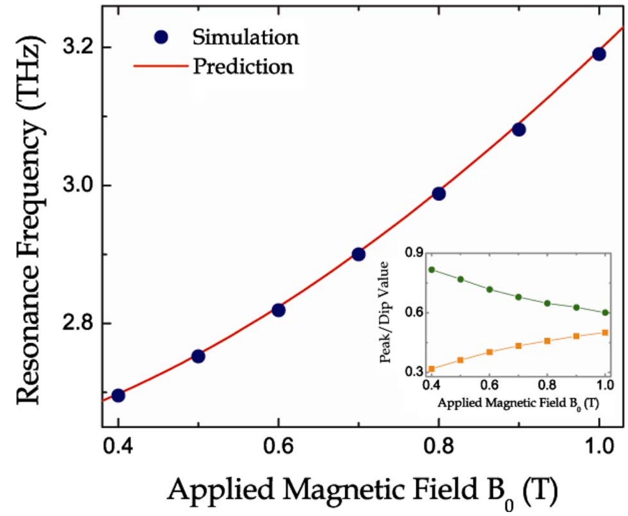


Fig. 2. (Color online) Dependences of the simulated and the analytically predicted values of the resonance frequency at 300 K on $B_0$. Inset, maximum $|r|$ and minimum $|t|$ as functions of $B_0$.

mentum [3,10]. Therefore, $\vec{k}=\vec{k}_\parallel+\vec{G}$, where $\vec{k}$ is the wave vector of the surface magnetoplasmons wave; $\vec{k}_\parallel$ is the in-plane component of the wave vector of the incident plane wave with $k_\parallel=\frac{\omega}{c}\sin\theta$, where $\theta$ is the angle of incidence with respect to the $x$ axis and $c$ is the speed of light in free space; and $\vec{G}$ is the reciprocal lattice vector whose magnitude is related to multiples of $2\pi/a_0$. When no holes are present, $\vec{k}$ satisfies the dispersion relation $\alpha+\alpha_0\varepsilon_V+ik(\varepsilon_{xz}/\varepsilon_{xx})=0$ [19], where $\alpha^2=k^2-(\omega^2/c^2)\varepsilon_V$, $\alpha_0^2=k^2-(\omega^2/c^2)\varepsilon_S$, and $\varepsilon_V=\varepsilon_{xx}-\varepsilon_{xz}^2/\varepsilon_{xx}$. The foregoing relations suffice to analytically predict the resonance frequency for each value of $B_0$.

The solid curve in Fig. 2 represents the analytically predicted resonance frequency, which is in good agreement with the simulated results. Being consistent with the simulated results, the analytical prediction clearly reveals that the magnetic tunability of the subwavelength-hole array originates from the excitation of surface magnetoplasmons. The enhancements in the peak of $|r|$ and the dip of $|t|$ can be understood as owing to the field enhancement of surface magnetoplasmons with increasing dc magnetic field.

Next, we present the thermal tunability of the chosen structure. In contrast to metals, the plasma frequency $\omega_p$ of InSb depends strongly on the temperature. When the temperature is between 250 and 320 K, the energy gap of InSb changes very little with temperature, and the intrinsic carrier density $N$ (in $\mathrm{cm}^{-3}$) can be described well by the relation $N=5.76\times10^{14}T^{3/2}\exp(-0.26/2k_BT)$ [20], where $k_B$ is the Boltzmann constant and the temperature $T$ is in kelvin. A variation in $N$ owing to a variation in $T$ thus changes $\omega_p$. Consequently, in the low-terahertz regime, $\hat{\varepsilon}(\omega)$ of is very sensitive to $T$. Hence, we can expect that temperature variations can induce substantial variations in the resonance characteristics of the chosen structure.

Finally, to demonstrate magnetothermal tunability, let us fix $B_0=0.5$ T, but change $T$ from 250 to

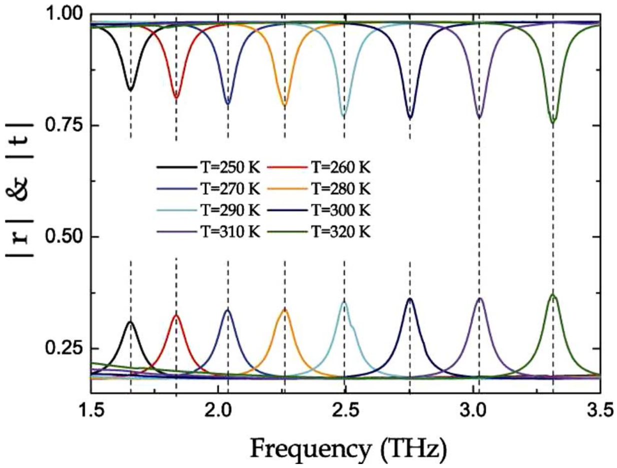


Fig. 3. (Color online) Simulated temperature-dependent spectra of $|r|$ (lower) and $|t|$ (upper) when $B_0 = 0.5$ T in magnitude. Note that $|r|^2 + |t|^2 < 1$.

320 K. Figure 3 shows that the resonance frequency then blueshifts from 1.65 to 3.31 THz—a shift of more than 100%. Whereas $N \sim 5.45 \times 10^{15}$ cm$^{-3}$ in InSb at 250 K, $N \sim 2.96 \times 10^{16}$ cm$^{-3}$ at 320 K, corresponding to the change in $\omega_p / 2\pi$ from 5.33 to 12.59 THz, as shown in the inset of Fig. 4. Hence, the excitation of surface magnetoplasmons must be seriously affected by the temperature.

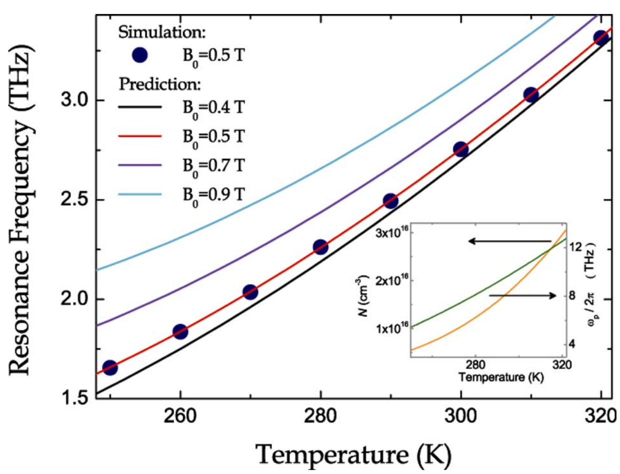


Fig. 4. (Color online) Solid circles indicate the values of the resonance frequency from the CST simulation, when $B_0 = 0.5$ T. The solid curves show the analytically predicted resonance frequency as a function of temperature for $B_0 = 0.4$, 0.5, 0.7, and 0.9 T. The inset shows the variations in $N$ and $\omega_p$ with $T$ when $B_0 = 0.5$ T.

The solid curves in Fig. 4 show the analytically predicted resonance frequencies, as the temperature changes from 250 to 320 K, while the dc magnetic field magnitude $B_0$ is held fixed at 0.4, 0.5, 0.7, and 0.9 T. For $B_0 = 0.5$ T, the predicted values are very consistent with the simulated results.

In summary, we have shown that there are three ways of blueshifting the resonance frequency of an array of subwavelength holes in a semiconductor sheet: (i) by increasing the magnitude of a dc magnetic field in a Voigt configuration, while holding the temperature fixed; (ii) by increasing the temperature, while holding the dc magnetic field magnitude fixed; and (iii) by increasing both the temperature and the dc magnetic field magnitude. The shifts obtainable can be very large.

## References

1. H. A. Bethe, Phys. Rev. **66**, 163 (1944).
2. A. Lakhtakia, M. F. Iskander, C. H. Durney, and H. Massoudi, IEEE Trans. Biomed. Eng. **29**, 569 (1982).
3. T. W. Ebbesen, H. J. Lezec, H. F. Ghaemi, T. Thio, and P. A. Wolff, Nature **391**, 667 (1998).
4. F. J. García de Abajo, Rev. Mod. Phys. **79**, 1267 (2007).
5. R. Gordon, J. Nanophotonics **2**, 020305 (2008).
6. J. G. Han, A. K. Azad, M. Gong, X. Lu, and W. Zhang, Appl. Phys. Lett. **91**, 071122 (2007).
7. Y. D. Liu and S. Blair, Opt. Lett. **28**, 507 (2003).
8. J. C. Sharpe, J. S. Mitchell, L. Lin, H. Sedoglavich, and R. J. Blaikie, Anal. Chem. **80**, 2244 (2008).
9. A. K. Azad, Y. Zhao, W. Zhang, and M. He, Opt. Lett. **31**, 2637 (2006).
10. J. Han, X. Lu, and W. Zhang, J. Appl. Phys. **103**, 033108 (2008).
11. J. Y. Suh, E. U. Donev, R. Lopez, L. C. Feldman, and R. F. Haglund, Jr., Appl. Phys. Lett. **88** 133115 (2006).
12. C.-L. Pan, C.-F. Hsieh, R.-P. Pan, M. Tanaka, F. Miyamaru, M. Tami, and M. Hangyo, Opt. Express **13**, 3921 (2005).
13. J. Gómez Rivas, P. Haring Bolivar, and H. Kurz, Opt. Lett. **29**, 1680 (2004).
14. W. Zhang, A. K. Azad, J. Han, J. Xu, J. Chen, and X.-C. Zhang, Phys. Rev. Lett. **98**, 183901 (2007).
15. Y. M. Strelniker and D. J. Bergman, Phys. Rev. B **59**, R12763 (1999).
16. Y. M. Strelniker, D. Stroud, and A. O. Voznesenskaya, J. Appl. Phys. **99**, 08H702 (2006).
17. S. C. Howells and L. A. Schlie, Appl. Phys. Lett. **69**, 550 (1996).
18. J. Han, A. Lakhtakia, and C.-W. Qiu, Opt. Express **16**, 14390 (2008).
19. J. J. Brion, R. F. Wallis, A. Hartstein, and E. Burstein, Phys. Rev. Lett. **28**, 1455 (1972).
20. J. Han and A. Lakhtakia, J. Mod. Opt. **56**, 554 (2009).